Free Vibration of Rectangular Plates with Two Symmetrically Distributed Clamps Along One Edge

Daniel J. Gorman*
University of Ottawa, Ottawa, Canada

In this paper the method of superposition is employed to compute the free vibration eigenvalues for a thin rectangular plate held in a cantilever configuration by a pair of clamps symmetrically distributed along one edge. Eigenvalues are tabulated for the limiting case when the clamp area approaches zero and the plate is supported by applied concentrated forces and moments. The method is equally applicable to cases where the clamps cover a finite area. Good agreement has been obtained when theoretical results are compared with those obtained experimentally. By means of a small modification to earlier computational practices it has been possible to greatly increase accuracy. The modification is described in detail.

Nomenclature

a,b	= dimensions of half-plate
D	= plate flexural rigidity $= Eh^3/12(1-\nu^2)$
E	= Young's modulus of plate material
h	= plate thickness
K,Kl	= upper limits used in series expansions
M	= amplitude of applied bending moment
M^*	= dimensionless applied moment amplitude, $= Mb^2/aD$
P	= amplitude of concentrated force
P^*	= dimensionless concentrated force amplitude, $= Pb^3/a^2D$
V	= distributed vertical edge reaction
W	= plate lateral displacement amplitude divided by dimension a
x,y	= plate spatial coordinates
ζ	= distance from plate centerline to support point divided by dimension a
ξ	$= x/a$
η	$= y/b$
ϕ	= half-plate aspect ratio, b/a
ϕ_p	= full-plate aspect ratio, $b/2a$
ω	= circular frequency of plate vibration
ρ	= mass of plate per unit area
λ^2	$= \omega a^2\sqrt{\rho/D}$
λ^{*2}	$= \omega b^2\sqrt{\rho/D}$
ϵ	= distance between concentrated forces divided by side length b
ν	= Poisson's ratio of plate material

Introduction

SOLUTIONS for the free vibration frequencies and mode shapes of rectangular plates with classical edge conditions are now well-known. Eigenvalues have been tabulated for all combinations of these edge conditions and a wide range of plate aspect ratios. There are, nevertheless, numerous rectangular plate free vibration problems that do not fall into the above category and are of interest to designers. Of particular interest is the problem of the free vibration of rectangular plates held in a cantilever configuration by means of a pair of rigid clamps distributed symmetrically along an edge. It is of interest to the European Space Agency because rectangular plates with similar support arrangement have a potential for use as solar energy collectors and antennas for space satellites.

It will be immediately appreciated that free vibration analysis of such a plate is not an easy task. Lateral displacement of the plate is forbidden at the support points. Furthermore, rotation of the plate in either principal direction, at the points of support, is also forbidden. In the idealized case, the condition of zero lateral displacement and rotation will be achieved by means of cyclic concentrated forces and moments, respectively. The problem differs from the classical cantilever plate problem because these forces and moments are concentrated rather than distributed. It will be seen that through a superposition of known rectangular plate forced vibration solutions, a solution to the free vibration problem of interest is obtained.

Analytical Procedure

Before beginning the analysis, it is important to note that, because of the symmetry in the clamp distribution, all of the modes of free vibration of the plate will be either symmetric, or antisymmetric, with respect to the central axis of the plate (Fig. 1). It is found to be advantageous to analyze these two families of modes separately. In fact, provided the boundary conditions are properly enforced, it is necessary to analyze only half of the plate when examining either family of modes.

Analysis of Symmetric Modes

We begin by considering the rectangular plate forced vibration solutions which are represented schematically in Fig. 2. Each solution will be referred to as a "building block" to be utilized in the superposition method employed here. The geometry of each building block coincides with that of the right half of the original plate (Fig. 1). Two small circles adjacent to any edge of a building block indicate a special type of boundary condition. This condition, which has already been discussed by the author,[1] is one where zero vertical edge reaction is permitted along the plate and where slope taken normal to the edge is everywhere zero.

In the case of the first building block in Fig. 2, i.e., the building block with displacement $W_1(\xi,\eta)$, there is a harmonic bending moment applied along the edge $n = 1$. This bending moment is represented in dimensionless form by a Fourier cosine series as

$$\frac{Mb^2}{aD} = \sum_{m=0}^{\infty} E_m \cos m\pi\xi \tag{1}$$

Received July 26, 1985; revision received Jan. 29, 1986.

*Professor, Department of Mechanical Engineering.

There is zero vertical edge reaction permitted along the edge, $\eta = 1$, and it is well known that an exact Lévy-type solution can be written for its steady-state response. Because the procedure for obtaining such solutions has been discussed in detail by the author in an earlier publication,[1] only the solution will be provided here in the interest of completeness. It is shown that this solution can be written as

$$W_1(\xi,\eta) = \sum_{m=0,1}^{K^*} \frac{E_m}{\theta_{11m}}\{\cosh\beta_m\eta + \theta_{1m}\cos\gamma_m\eta\}\cos m\pi\xi + \sum_{m=K^*+1}^{\infty} \frac{E_m}{\theta_{22m}}\{\cosh\beta_m\eta + \theta_{2m}\cosh\gamma_m\eta\}\cos m\pi\xi \quad (2)$$

where

$$\beta_m = \phi\sqrt{\lambda^2 + (m\pi)^2}$$

$$\gamma_m = \phi\sqrt{\lambda^2 - (m\pi)^2} \quad \text{or} \quad \phi\sqrt{(m\pi)^2 - \lambda^2}$$

whichever is real, and the first series contains only those terms for which $\lambda^2 > (m\pi)^2$. Symbols θ_{11m}, θ_{1m}, etc., are defined in Ref. 1.

Solutions for the second and third building blocks can be readily extracted from the above solution; it is only necessary to introduce a change in coordinates to obtain the second solution.[1] The third solution can be obtained by replacing the variable η of the first solution with the quantity $1-\eta$. Solutions of this type have been used extensively by the author in analyzing completely free rectangular plates.[2]

We turn next to the problem of choosing building blocks which permit the elimination of displacement and slope at the point of support. Elimination of the displacement presents no difficulty. This is accomplished by means of the fourth building block in Fig. 3 in a manner identical to that described by the author in Ref. 3. The nondriven edges of this block have support identical to those of the first building block. Along the driven edge a condition of zero bending moment is imposed. The edge is driven harmonically by a concentrated force which is represented in dimensionless form by means of the Dirac delta function[3]

$$\frac{V(\xi)b^3}{a^2D} = P^* \sum_{m=0,1}^{\infty} \frac{2\cos m\pi\zeta}{\delta_m}\cos m\pi\xi \quad (3)$$

where

$$\delta_m = 2, \quad m = 0; \quad \delta_m = 1, \quad m \neq 0$$

and $P^* = (Pb^3/a^2D)$, the dimensionless concentrated force. The solution for the building block is shown to be

$$W_4(\xi,\eta) = \sum_{m=0,1}^{K^*} P^* C_{1m}(\cosh\beta_m\eta + \theta_{1m}\cos\gamma_m\eta)\cos m\pi\xi + \sum_{m=k^*+1}^{\infty} P^* C_{2m}(\cosh\beta_m\eta + \theta_{2m}\cosh\gamma_m\eta)\cos m\pi\xi \quad (4)$$

where, because there is zero bending moment along the driven edge, the quantities θ_{1m} and θ_{2m} must be identical to those of Eq. (2). The quantities C_{1m} and C_{2m} are defined in Ref. 3.

Finally, it is necessary to consider the problem of eliminating slope at the point of support. It is logical to begin by exploring the possibility of utilizing building blocks with concentrated bending moments at the support point. Building blocks of this type have been discussed in detail in Ref. 4. Unfortunately, it is found that utilization of such building blocks is not permissible in the problem under study as their introduction would immediately cause convergence problems. It is well known that series which normally converge may present problems when the derivative of the function they represent is required. When we introduce a concentrated moment, rather than a concentrated force, we already aggravate the convergence problem.[5] This is because the concentrated force involves a higher order of derivative and hence more integration to obtain the displacement solution. To aggravate the situation even more, we are interested in the slope, i.e., the first spatial derivatives of the displacement, rather than the displacement itself, at the point of application of the moment. It can be shown that the series thus obtained for this slope does not, in fact, converge. We are forced, therefore, to look at alternate methods to handle the problem of elimination of slope at the point of support.

We consider the case of a thin uniform beam with simple support conditions (zero displacement and zero moment) at each end. Let there be another simple support located at an intermediate position along the beam. This latter support prevents displacement at its point of application but does not impose any moment on the beam. The solution for this double span beam problem is well known. It is also known that as the intermediate support is allowed to approach arbitrarily close to either end support, the beam natural frequencies approach those of a clamped simply supported beam. The two adjacent but distinct supports ensure zero displacement of the beam end and also serve to eliminate slope in this region. In fact, by computing eigenvalues of the beam for successively diminishing distances between the adjacent supports and using a linear extrapolation process one arrives at the known eigenvalue for the clamped simply in supported beam.

The identical process has been utilized for the plate problem under study here. Examining the fifth building block in Fig. 2, it is seen that it differs from the fourth building block only in that the concentrated force is applied at a small dimensionless distance ϵ from the plate edge. The solution for the fifth building block is almost identical to one developed in Ref. 6. The only difference is that here we wish to enforce the conditions of zero bending moment along edges parallel to the ξ axis instead of the conditions of zero slope imposed in the earlier publication.

It is shown that the solution for the region $\eta \leq (1-\epsilon)$ may be written as

$$W_{51}(\xi,\eta) = \sum_{m=0,1}^{K^*} P^*[A_m(\cosh\beta_m\eta + \theta_{1m}\cos\gamma_m\eta) + B_m(\sinh\beta_m\eta + \phi_{2m}\sin\gamma_m\eta)]\cos m\pi\xi + \sum_{m=K^*+1}^{\infty} P^*[A_{mm}(\cosh\beta_m\eta + \phi_{1mm}\cosh\gamma_m\eta) + B_{mm}(\sinh\beta_m\eta + \phi_{2mm}\sinh\gamma_m\eta)]\cos m\pi\xi \quad (5)$$

where the first summation includes only terms for which $\lambda^2 > (m\pi)^2$. All of the quantities, A_m, B_m, θ_{1m}, etc., are determined once the plate geometry and location of the driving force are selected.[6] The solution for the region $\eta > (1-\epsilon)$ can be extracted from the above solution because of the symmetry in the problem.

Finally, the sixth building block, which is required to eliminate slope at the support point in the direction parallel to the ξ axis, will have a form identical to that of the fourth building block. With these building block solutions available, we are now in a position to obtain a solution for the free vibration symmetric modes of the plate in Fig. 1.

Analysis of Antisymmetric Modes

Only a brief description of the building blocks utilized in analyzing the antisymmetric modes will be given. This is because these building blocks differ in only one way from those of Fig. 2. It will be appreciated that boundary conditions to be imposed along the η axis for antisymmetric mode analysis will be of zero displacement and zero bending moment. This is readily achieved by using Lévy solutions ex-

pressed as

$$W(\xi,\eta)=\sum_{m=1,3,5}^{\infty} Y_m(\eta)\sin\frac{m\pi\xi}{2} \tag{6}$$

for all building blocks except the second one. For the second building block the solution will differ from that employed in the symmetric mode analysis since simple support conditions must be enforced along the edge $\xi=0$.

Computation of Eigenvalues

The computation procedure will be essentially the same whether symmetric or antisymmetric modes are under investigation. We will focus our discussion on analysis of the symmetric modes.

The procedure followed is similar to that described in earlier publications. The requirement that there should be zero net moment along three of the edges of the superimposed building blocks leads to the generation of $3K$ linear homogenous algebraic equations where K is the number of terms utilized in the series representing the moments. In each case, the moment along one edge exists in series form. Moments along the other edges are expanded in the same series. Three additional algebraic equations are obtained by enforcing the condition of zero net displacement at the points of application of the concentrated forces.

The coefficient (eigenvalue) matrix thus generated is shown schematically in Fig. 3, where, for simplicity, a value of three has been used for the limit K. It will be noted that many elements of the matrix need not be computed since they equal zero. Computation is further simplified by taking advantage of symmetry. The first three sets of equations arise because of the requirement of zero net moment along the edges $\eta=1$, $\xi=1$, and $\eta=0$, respectively. This is indicated by the small rectangular blocks adjacent to the matrix. The final three equations express the condition of zero net displacement at points indicated in the small rectangles to the lower right of the matrix.

In earlier computations involving concentrated forces the author has found it necessary to use very large matrices in order to obtain satisfactory accuracy in the results. A new feature has been introduced into the computations here which has permitted the same degree of high accuracy without requiring the same large matrices. Building blocks in which the Dirac function is employed will normally require a high number of terms in their series in order to obtain satisfactory convergence. On the other hand, satisfactory accuracy can be obtained while using fewer terms in the first three building blocks which do not utilize this function. With the upper limit for the series representing the applied distributed moments designated by the letter K it will be evident that the matrix size will be $3\ (K+1)$ by $3(K+1)$. The upper limit for the series representing the concentrated forces is designated by the symbol Kl. It is advantageous to set Kl much larger than K; however, the terms lying between K and Kl will affect only those elements found in the mid section and lower section of the three right hand columns of the matrix. These two regions of the matrix are blocked off by heavy lines in Fig. 3.

It is found that modification to the computation procedure vastly reduces required computer storage area and facilitates the provision of high accuracy in displacement calculations at the points of support. It is obvious that such accuracy is required at these points. For the symmetric modes a value of $Kl=200$ was utilized while, for the antisymmetric modes, the value of Kl was set equal to 300. In the latter case only odd values of the subscript m are utilized. It was found that these values for the series limits gave the required three-digit accuracy.

A further decision that had to be made relates to the value of the dimensionless quantity, ϵ. After numerous tests it was decided to make a quadratic rather than a linear extrapolation in order to obtain more accuracy in the eigenvalues. This necessitated making computations for three different values of ϵ. The values selected were 0.006, 0.004 and 0.002.

One further comment should be made about the computations. It was decided to investigate the effect of introducing an additional building block, essentially identical to the fifth building block in Fig. 2. The concentrated force of this latter building block would act at a distance $\epsilon/2$ from the plate edge. This would be analogous to utilizing two intermediate supports in the beam problem discussed previously and letting both supports approach one end. It was found that introduction of this extra building block did not significantly affect the computed results, but it was retained for all of the computations.

Presentation of Results

While numerous researchers have analyzed the vibration of plates with point supports (see review by A.W. Leissa[7]) the author is aware of no published results related to the problem under consideration here. It was evident, therefore, that a comparison could not be made with results of other studies. Accordingly, it was decided to perform a limited number of experimental tests. The experimental apparatus utilized is shown in Fig. 4. A rectangular aluminum plate of 0.080 in. (2.03 mm) thickness was mounted on a test base which, in turn, was mounted on an electrodynamic shaker. The plate

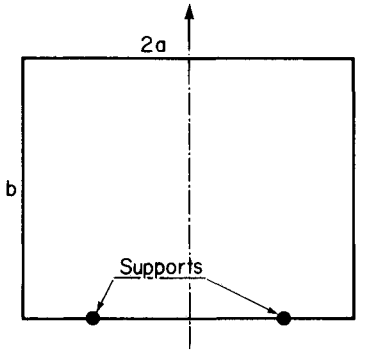

Fig. 1 Rectangular plate with two symmetrically distributed edge supports. Displacement and slope (normal and parallel to edge) are forbidden at supports.

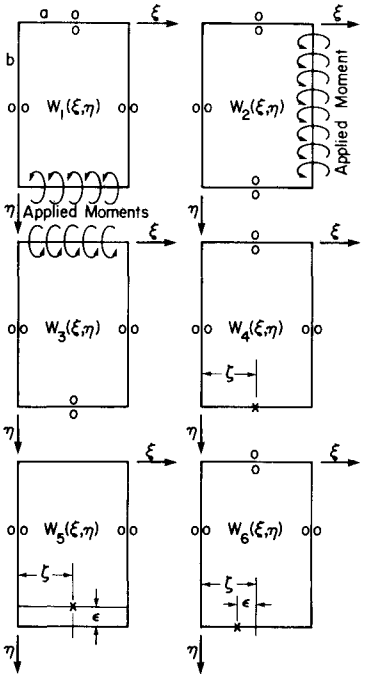

Fig. 2 Building blocks utilized in symmetric mode analysis. X indicates point of force application and ζ indicates dimensionless distance from centerline to support.

Table 1 Comparison of symmetric mode experimental and theoretical free vibration frequencies for square [12×12 in. (30.5×30.5 cm)] aluminum plate

	First mode (Hz)		Second mode (Hz)	
ζ	Theoretical	Experimental	Theoretical	Experimental
0.25	14.6	15.2	83.1	84.1
0.50	15.0	15.1	99.1	98.2
0.75	14.2	15.2	97.4	104.6

Table 2 Comparison of symmetric mode experimental and theoretical free vibration frequencies for a rectangular [12×18 in. (30.5×45.7 cm)] aluminum plate[a]

	First mode (Hz)		Second mode (Hz)	
ζ	Theoretical	Experimental	Theoretical	Experimental
0.25	10.2	10.0	65.7	64.0
0.50	10.6	10.4	68.7	67.7
0.75	10.1	10.0	67.3	67.8

[a]Clamps are located along shorter edge.

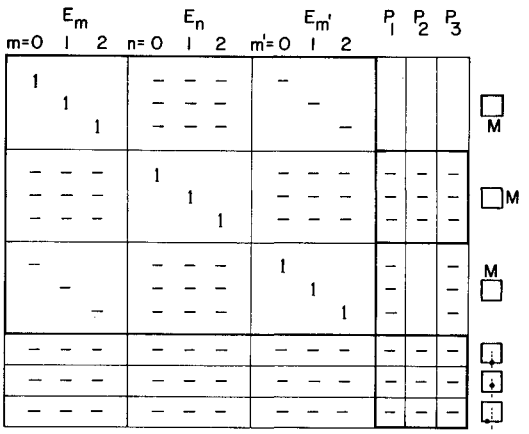

Fig. 3 Schematic representation of eigenvalue matrix based on three-term series expansions.

was fixed to the base by two symmetrically distributed clamps (see Fig. 4). The jaws of each clamp were 0.375 in. (0.953 cm) in width and they protruded 0.375 in. onto the plate surface. After assembly, the clamps were tightened rigidly with heavy bolts. The clamps could be located at any desired position along the edge of the plate. In a typical test the base holding the plate was made to undergo low-amplitude harmonic motion while the frequency was gradually increased. The motion of the plate was monitored by means of a strain gage shown in the figure. Following this procedure, the resonant frequencies of the plate could be obtained and compared with those obtained theoretically.

In computing eigenvalues, and hence frequencies, for the experimentally tested plates, it was not necessary to use any limiting process. In fact, this is always true when utilizing the theoretical approach described here so long as the clamps cover a finite area of the plate.

Comparison of Theoretical and Experimental Results

Results of experimental tests conducted on a 12×12 in. (30.5 cm) square aluminum plate of 0.080 in. (2.03 mm) thickness are tabulated in Table 1. Results of theoretical studies performed for the same plate are also presented. The first- and second-lateral vibration modes were studied for three different separation distances between the clamps.

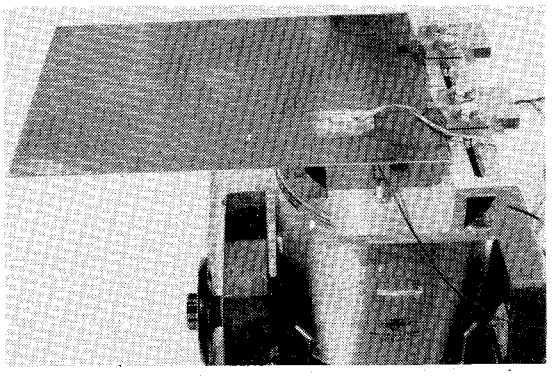

Fig. 4 View of aluminum plate with two clamp supports mounted on shaker test facility.

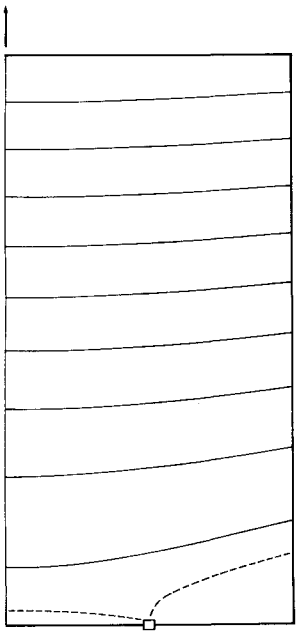

Fig. 5 Contour plot of mode shape for first symmetric mode vibration of square plate, $\zeta=0.5$. Broken line indicates node line.

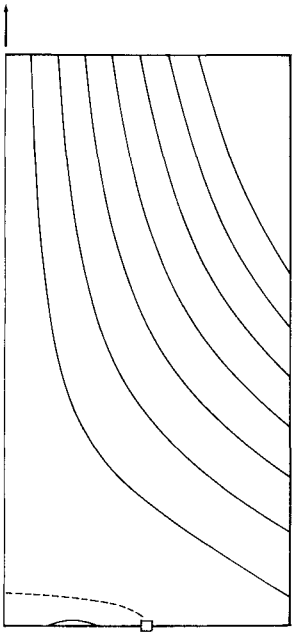

Fig. 6 Contour plot of mode shape for first antisymmetric mode vibration of square plate, $\zeta=0.5$. Broken line indicates node line.

Table 3 Computed eigenvalues for first and second symmetric mode free vibration

		$\lambda^2 = \omega a^2\sqrt{\rho/D}$, $\phi_p = b/2a$										
ζ	Mode	1/3.0	1/2.5	1/2.0	1/1.5	1/1.25	1.0	1.25	1.5	2.0	2.5	3.0
0.25	1	2.54	1.97	1.40	0.891	0.665	0.464	0.322	0.238	0.138	0.100	0.0730
	2	5.33	5.08	4.89	4.60	4.25	3.45	2.48	1.81	1.07	0.703	0.499
0.50	1	2.70	2.03	1.42	0.899	0.672	0.469	3.26	0.242	0.149	0.101	0.0737
	2	6.47	6.27	6.05	5.75	5.32	3.94	2.63	1.87	1.08	0.708	0.501
0.75	1	2.54	1.94	1.38	0.874	0.654	0.457	0.318	0.236	0.146	0.0995	0.0722
	2	6.68	6.34	6.06	5.77	5.47	4.00	2.66	1.88	1.08	0.706	0.499
1.00	1	1.67	1.31	0.954	0.623	0.472	0.336	0.238	0.179	0.114	0.0796	0.0592
	2	5.43	5.02	4.70	4.32	4.03	3.34	2.41	1.74	1.01	0.660	0.465

Table 4 Computed eigenvalues for first and second antisymmetric mode free vibration

		$\lambda^2 = \omega a^2\sqrt{\rho/D}$, $\phi_p = b/2a$										
ζ	Mode	1/3.0	1/2.5	1/2.0	1/1.5	1/1.25	1.0	1.25	1.5	2.0	2.5	3.0
0.25	1	3.14	2.76	2.33	1.86	1.60	1.32	1.09	0.929	0.717	0.584	0.492
	2	11.3	10.0	8.59	6.87	5.86	4.76	3.81	3.16	2.35	1.87	1.55
0.50	1	4.80	4.01	3.23	2.42	2.02	1.61	1.29	1.07	0.799	0.637	0.530
	2	13.6	12.8	11.5	9.23	7.62	5.88	4.51	3.64	2.61	2.03	1.67
0.75	1	6.19	5.03	3.88	2.80	2.29	1.80	1.41	1.15	0.844	0.666	0.550
	2	16.5	16.2	15.8	11.8	9.06	6.63	4.93	3.92	2.76	2.13	1.73
1.00	1	5.78	4.65	3.60	2.66	2.20	1.71	1.37	1.13	0.834	0.662	0.547
	2	15.0	14.8	13.7	11.0	8.69	6.48	4.86	3.82	2.71	2.11	1.72

Because of space limitations on the test base it was not possible to move the support clamps to the extreme outer corners.

The differences between theoretical and experimental frequencies are generally within about 5 or 6% and are sometimes even less. This probably can be considered as fairly good agreement in view of the formidable problems involved in trying to model the support conditions, both experimentally and theoretically.

Experimental and theoretical studies were also conducted for a rectangular aluminum plate of 12×18 in. (30.5×45.7 cm) and 0.080 in. (2.03 mm) thickness. The clamps were symmetrically distributed along a short edge; these results are tabulated in Table 2. It is seen that there is very good agreement between experiment and theory of this plate.

Tabulation of Computed Eigenvalues

Eigenvalues have been computed for first- and second-mode free vibration of rectangular plates in symmetric and antisymmetric mode vibration. These results, presented in Tables 3 and 4, have been prepared for a wide range of full-plate aspect ratios and for four different dimensionless separation distances of the edge clamps.

All of the results have been obtained by the extrapolation procedure discussed earlier. The computed eigenvalues pertain to limiting cases where motion of the plate at the clamps is prevented by concentrated forces and concentrated moments. They have been prepared with a view to providing three-digit accuracy. In many real problems the clamping area will spread over a limited region of the plate. This will have the effect of slightly increasing the plate free vibration frequencies.

A contour plot of the mode shape for first symmetric mode free vibration of a square plate is presented in Fig. 5. Because of symmetry, it is necessary to show only half of the plate. A similar plot for the first antisymmetric mode of the same plate is presented in Fig. 6. In each case the left vertical line represents the centerline of the plate.

Summary and Conclusions

Through a judicious choice of building blocks it has been possible to utilize the superposition method to obtain an analytical type solution for a rather difficult rectangular plate free vibration problem. As indicated earlier, plates of this type have application in the aerospace industry. The analytical procedures described here can be readily modified to obtain conditions that vary somewhat from those described. As long as the problem is linear in nature, its solution is dependent only on the ingenuity of the analyst.

A substantial improvement in the computation procedure was achieved when it was decided to explore the possibility of increasing the number of terms used in those building block solutions where concentrated forces were involved. The result was the achievement of much higher accuracy without increasing the matrix size. This procedure will be followed in future computational work.

References

[1]Gorman, D.J., "Free Vibration Analysis of the Completely Free Rectangular Plate by the Method of Superposition," *Journal of Sound and Vibration,* Vol 57, April 1978, pp. 437–447.

[2]Gorman, D.J., *Free Vibration Analysis of Rectangular Plates,* Elsevier North Holland, Inc., New York, 1982.

[3]Gorman, D.J., "Free Vibration Analysis of Rectangular Plates with Symmetrically Distributed Point Supports Along the Edges," *Journal of Sound and Vibration,* Vol. 73, No. 4, Dec. 1980, pp. 563–574.

[4]Gorman, D.J., "Dynamic Response of a Rectangular Plate to a Bending Moment Distributed Along the Diagonal," *AIAA Journal,* Vol. 20, Nov. 1982, pp. 1616–1621.

[5]Gorman, D.J., "On Use of the Dirac Delta Function for Representing Concentrated Forces and Moments in Structural Mechanics," *International Journal of Mechanical Engineering Education,* Vol. 10, March 1982, pp. 177–183.

[6]Gorman, D.J., "An Analytical Solution for the Free Vibration Analysis of Rectangular Plates Resting on Symmetrically Distributed Point Supports," *Journal of Sound and Vibration,* Vol. 79, No. 4, Dec. 1981, pp. 561–574.

[7]Leissa, A.W., "Vibration of Plates," NASA SP-160, 1969.